Wang, R., Woith, H., Milkereit, C., Zschau, J. (2004): Modelling of hydrogeochemical anomalies induced by distant earthquakes. - Geophysical Journal International, 157, 2, pp. 717—726.

DOI: http://doi.org/10.1111/j.1365-246X.2004.02240.x

Geophys. J. Int. (2004) **157,** 717–726 doi: 10.1111/j.1365-246X.2004.02240.x

Modelling of hydrogeochemical anomalies induced by distant earthquakes

Rongjiang Wang, Heiko Woith, Claus Milkereit and Jochen Zschau

GeoForschungsZentrum Potsdam (GFZ), Telegrafenberg, D-14473 *Potsdam, Germany. E-mail: wang@gfz-potsdam.de*

Accepted 2003 November 25. Received 2003 November 13; in original form 2003 April 15

SUMMARY

By analysing several years of discharge and electrical conductivity data from an artesian well in Kajaran, Armenia, we found a significant sensitivity of this well to distant large earthquakes. In general, the discharge increases co-seismically and the conductivity decreases post-seismically with a time delay of about 1 hr. The post-seismic trends of the conductivity reach a minimum after about 3 weeks and then need several months to recover to the pre-seismic level. For instance, the $M_w = 7.6$ Izmit earthquake in Turkey on 1999 August 17, at a distance of 1400 km, led to an increase of 25 per cent in discharge and a decrease of up to 6 per cent in conductivity. The discharge also shows tidal fluctuations of amplitude roughly 5 per cent (peak-to-peak) of the mean well production, whereas the tidal signal in the conductivity data is less significant and unstable. The maximum co-seismic static strain estimated for 11 earthquakes that induced an anomaly during the monitoring period is below 10^{-9}, or at least one order smaller than the tidal strain. Therefore, the well-water anomalies related to the distant earthquakes are believed to be induced by seismic ground shaking rather than co-seismic deformation. We suggest mixing of groundwater as an explanation for the observations and present a model which considers specific conditions for this particular groundwater system: a confined aquifer with a high contrast in the hydrogeochemical composition between two different groundwaters and a macrofracture as the mixing zone which is hydraulically connected to the artesian well. The earthquake-related anomalies are believed to result from a local head increase near the artesian well, induced by the passage of seismic waves. Possible mechanisms are discussed, and the time histories of the anomalies are modelled.

Key words: Armenia, earth tides, groundwater anomalies, Izmit earthquake, modelling, Turkey.

1 INTRODUCTION

It has long been known that earth tides, barometric loads or seismic waves can induce measurable periodic fluctuations in water level in certain wells (Bredehoeft 1967; Sterling & Smets 1971; Igarashi & Wakita 1991; Ohno *et al.* 1997). These phenomena are believed to reflect dilatations or compressions of confined and transmissive aquifers to which the wells are connected. Similarly, co- and post-seismic aperiodic changes in physico-chemical groundwater parameters (well-water level or discharge, temperature, radon concentration, etc.) within a few source dimensions of an earthquake faulting area have often been interpreted as the poroelastic response to co-seismic changes in static strain (Wakita 1975; Muir-Wood & King 1993; Quilty & Roeloffs 1997; Grecksch *et al.* 1999).

However, such an interpretation usually fails for another class of hydrogeological anomalies, namely post-seismic rising or dropping of groundwater levels, discharges and temperatures as well as electrical conductivities caused by earthquakes several hundred to a thousand kilometres away (Mogi *et al.* 1989; Kitagawa & Koizumi 1996; Kitagawa & Matsumoto 1996; Roeloffs 1998; Woith *et al.* 2001, 2003a; Brodsky *et al.* 2003).In most cases, the anomalies are monotonic and persist for up to several months. The co-seismic changes in static strain cannot explain such phenomena, because the anomalies are often much larger than would be expected and are always of uniform sign, independent of the focal mechanism of the earthquakes. Therefore, this kind of groundwater anomaly is believed to be induced by seismic waves. In previous publications it has been proposed that, under certain site conditions, ground shaking due to the arrival of seismic waves may induce permanent changes in local hydraulic properties and pore pressure. For instance, strong ground shaking due to local earthquakes may increase the permeability of shallow materials by opening partially cemented fractures (Rojstaczer & Wolf 1992; Rojstaczer *et al.* 1995). Roeloffs (1998) suggested that permeability changes can also be induced by distant earthquakes, but in other ways: low-amplitude shaking may be able to mobilize gas bubbles lodged in the pore space, restoring the reduced permeability. For fractured rocks

with poor gas in the pore fluid, Brodsky *et al.* (2003) claimed that seismically induced flow may remove barriers from fractures and restore the hydraulic connections there.

In this paper we will analyse 4 yr (1996–1999) of multiparameter monitoring data at an artesian (i.e. free-flowing) well in Kajaran (KAT), Armenia. Two parameters, the well discharge and the specific electrical conductivity of the well water flowing out, showed significant responses to earthquakes up to 1400 km away. Woith *et al.* (2001, 2003a) have already reported some of the observations and Woith *et al.* (2003b) presented the complete data. In particular, the observed anomalies in the two well-water parameters show not only changes in the groundwater head but also changes in its geochemical composition because the electrical conductivity is a proxy for total dissolved solids in the well water. In this paper we present a mixing model which considers the specific conditions at the observation site. We show that the model is able to explain the high sensitivity of the KAT groundwater system to earthquakes and predict its characteristic response time history.

2 THE OBSERVATIONAL DATA

The multiparameter monitoring system installed at KAT is part of the international earthquake research project READINESS (Realtime Data Information Network in Earth Sciences; Woith *et al.* 1998). Details about the technical setting of the station were given by Woith *et al.* (2003b). Fig. 1(a)shows the specific electrical conductivity of the well water from April 1996 to the end of 1999. In this period, there were 11 earthquakes which induced static strain changes larger than 10^{-11} at the observation site (Table 1). At least eight of them, namely EQ 2, 4, 6, 7, 8, 9, 10 and 11, were accompanied by clearly visible conductivity anomalies: the signal sometimes starts with a sudden decrease. The decreasing trend continues in the post-seismic phase and reaches its minimum after about 3 weeks. Then the curve slowly recovers to its pre-seismic level within several months. Seasonal variations in the conductivity data were not significant.

In September 1998, the monitoring system was supplemented by a flowmeter installed in a bypass which measures a quarter of the total well discharge of about 7.2 litre per minute. The flowmeter data are shown in Fig. 1b. In contrast to the conductivity parameter, the discharge parameter shows a significant seasonal variation of up to ± 30 per cent (Fig. 1b). The signature of the $M_w = 7.6$ Izmit earthquake in Turkey (EQ 10) on 1999 August 17 was visible in both well-water parameters, although the epicentre of the event is 1400 km distant from the observation site. The other three earthquakes, EQ 8, 9, and 11, which also occurred after the installation of the flowmeter, were visible in the conductivity data, but could not be clearly identified from the discharge data.

The spectral analysis has shown that in the first two monitoring years, 1996 and 1997, the main diurnal constituents (O_1 and S_1) and the main semi-diurnal constituents (M_2 and S_2) of earth tides were clearly visible in the conductivity data, but their amplitudes varied strongly with time. The maximum peak-to-peak amplitude observed was about 3.0 μS cm^{-1}, or 0.2 per cent (all constituents of the tidal band summed) of the mean conductivity value (Fig. 2a).After 1997 the tidal signal decreased steadily with time (Fig. 2b). In 1998, it was below the detectable spectral level of 0.1 μS cm^{-1} or 0.01 per cent (Fig. 2c), but in 1999, the diurnal S_1 and the semi-diurnal S_2 constituents appeared again (Fig. 2d). In comparison, earth tides in the discharge were more significant and their amplitudes did not vary that much. The peak-to-peak amplitude reached 5.0 per cent of the mean well discharge (Figs 2e and f).

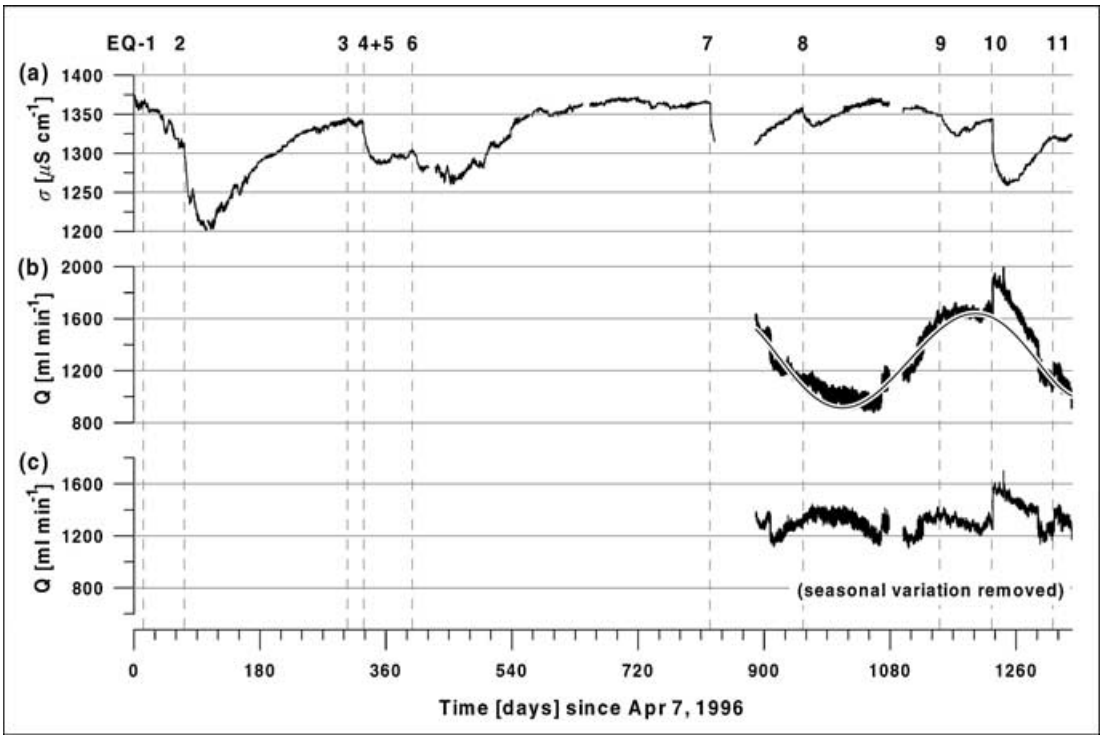

Figure 1. Observational data from the KAT artesian well (39.16°N, 46.21°E) near Kajaran, Armenia. (a) The specific electrical conductivity of the well water. (b) The well-water discharge from the flowmeter bypass that measures a quarter of the total well production (the superimposed sinusoidal curve represents a fit of the seasonal variation). (c) The well discharge rate corrected for the seasonal variation. Numbers at the top denote earthquakes (see Table 1).

Table 1. Earthquakes which induced a measurable anomaly in the well-water conductivity at the KAT station (39.16°N, 46.21°E). R is the distance of the epicentre from the KAT site, ϵ_v is the static volume strain based on the dislocation theory (+ dilatation, − compression, and ± max. possible dilatation or compression for earthquakes with $M_w < 5$ and thus without moment tensor solution), $\delta\sigma_o$ the maximum post-seismic conductivity drop, and σ_o the mean conductivity of the well water (∼1350 μS cm^{-1}). Earthquake data are taken from the Harvard CMT Catalog ($M_w \geq 5$ with moment tensor solution) and from the PDE Catalog of the USGS ($M_w < 5$ without moment tensor solution).

EQ No	M_w	Date	Lat. (°N)	Long. (°E)	R (km)	ϵ_v (10^{-9})	$\delta\sigma_o$ (per cent σ_o)
1	4.8	1996/04/22	39.17	47.37	100	±0.08	1.1
2	4.3	1996/06/18	39.16	45.80	35	±0.05	8.1
3	6.5	1997/02/04	37.82	57.50	993	−0.02	0.4
4	6.1	1997/02/28	38.03	48.06	187	+0.75	3.7
5	5.3	1997/03/02	37.86	47.87	204	+0.04	0.4
6	7.2	1997/05/10	33.58	60.02	1381	−0.07	1.5
7	5.9	1998/07/09	38.79	49.24	265	+0.08	6.7
8	4.8	1998/11/18	38.37	45.17	126	±0.01	1.5
9	5.4	1999/06/04	40.58	47.62	199	−0.03	1.9
10	7.6	1999/08/17	41.01	29.97	1395	+0.02	6.0
11	7.1	1999/11/12	40.93	31.25	1287	+0.02	0.7

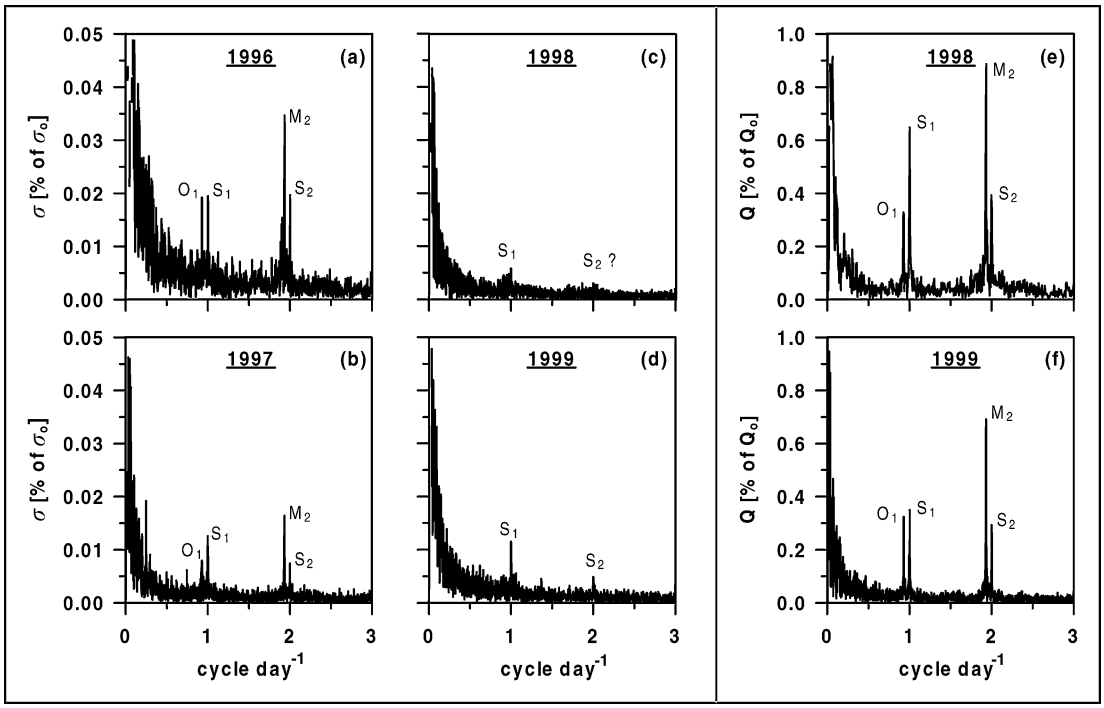

Figure 2. Spectral analysis of groundwater parameters at KAT. (a)–(d) Amplitude spectra of the specific electrical conductivity of the well water in per cent of the mean conductivity for the years 1996 to 1999, respectively. (e), (f) Amplitude spectra of the discharge rate in per cent of the mean well production for the years 1998 and 1999 respectively.

3 MODELLING OF MIXING PROCESSES IN THE KAT GROUNDWATER SYSTEM

3.1 The specific site conditions

The borehole was drilled 30 yr ago for scientific purposes and is 147 m deep. At about 80 m depth, it penetrates a macrofracture zone, possibly a tectonic fault. Groundwater might enter from there into the borehole. The well water flowing out includes a few per cent (volumetric content) of free CO_2 gas. Based on the analysis of groundwater samples at different locations near the borehole, Woith *et al.* (2003a) postulated that the well water is a mixture of 80–90 per cent shallow groundwater with 10–20 per cent deep, gas-rich (CO_2) fluid. The shallow groundwater is less conductive than the deep fluid. Woith *et al.* (2003a) estimated their conductivity contrast to be about 900 μS cm^{-1} to 4400 μS cm^{-1}. The former is comparable with the values shown by shallow water samples taken in the vicinity of the well, while the latter is the value of the well water from a neighbouring borehole which has the same depth as KAT but is known not to be connected to the shallow groundwater. A recent productivity test showed that the fracture zone is highly transmissive. In this test, the discharge of KAT was measured for different levels of the outflow tube. After each change in level, the well discharge reached a new equilibrium value exponentially within a few tens of minutes. The head pressure in the fracture zone was

been estimated to be about 20 kPa; that is, if the outflow tube were to be put more than 2 m higher than its original place during the monitoring time, no water would flow out.

3.2 A possible scenario for the earthquake-induced perturbation

Woith *et al.* (2003b) have found strong evidence that the conductivity anomalies related to the 11 earthquakes were not induced by co-seismic changes in static strain. First, all anomalies have an uniform negative sign, i.e. the conductivity always dropped, independently of the focal mechanism of the earthquakes. Among these 11 events, there were eight major earthquakes with magnitudes $M_w > 5$ for which the focal mechanism is known. If the phenomena were due to responses of the groundwater systems to changes in static strain we should have observed both positive and negative anomalies because three of the major earthquakes induced a compression and the other five induced a dilatation of the aquifer volume at the KAT site (Table 1). Secondly, the effects are too large to be readily expected from the static strain. In fact, the static volume strains estimated for the 11 events are all below 10^{-9}, or at least one order smaller than the volume strain caused by earth tides, but the induced anomalies are several orders larger than the amplitude of tidal fluctuations.

When a change in pore pressure is induced by the passage of seismic waves, the well discharge will react nearly co-seismically because of the high transmissivity of the fracture zone. If the spatial distribution of the change in pore pressure is not homogeneous but more or less localized, the mixing ratio between the two different groundwaters will also be perturbed, and the conductivity of the water mixture will consequently change. For example, Woith *et al.* (2003a) found that after the Izmit event (EQ 10), the mixing ratio was shifted by up to 2 per cent in favour of the shallow groundwater. Additionally, they showed evidence that the macrofracture zone at 80 m depth is most possibly the mixing location of the two different groundwaters. We therefore suggest the following scenario for the mixing process: in the unperturbed situation, the flow in the macrofractures starts with the shallow groundwater. On the way to the borehole, it 'picks up' the rising deep fluid, so that the conductivity of the flowing groundwater mixture increases from 800–900 μS cm^{-1} to 1300–1400 μS cm^{-1} when it arrives at the borehole. When the pore pressure in the shallow aquifer or the permeability of the fracture zone is suddenly increased, more fresh groundwater will be injected into the borehole and the well discharge will immediately rise. On the other hand, the increased head in the fracture zone can block the deep fluid from rising up. Consequently, the conductivity of the groundwater mixture drops.

The form of the signal of the conductivity anomalies depends not only on how the pore pressure is perturbed in space and time, but also on the spatial distribution of mixing locations. The farther the mixing locations from the borehole, the later is the signature of the perturbations seen by a sensor at the surface. In general, the conductivity anomalies first show a concave increase and then a long-term smooth recovery trend (Fig. 1a). This kind of spoon-like signal form may supply information which will help in understanding the groundwater mixing process.

3.3 A simple model for the background mixing process

In this section we will present a groundwater mixing model based on the qualitative analysis above. A sketch of the model is shown in Fig. 3.The artesian well penetrates a horizontal macrofracture zone at a depth of 80 m; this is supposed to be hydraulically connected to a shallow groundwater body. The medium beneath the fracture is a rock with microfractures where the mineralized deep fluid rises up.

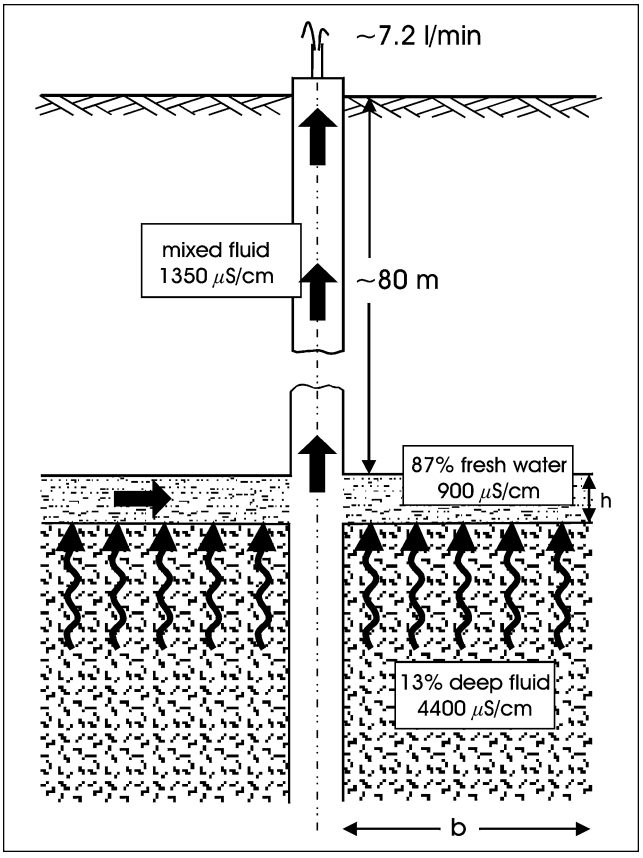

Figure 3. Sketch of the groundwater mixing model for the KAT observation site. The artesian well penetrates a horizontal macrofracture zone at a depth of about 80 m. The fracture zone is hydraulically connected to a shallow aquifer. The flow in the fracture starts from a distant place with fresh water of low conductivity (900 μS cm^{-1}). In an area around the well, conductivity is enhanced by the highly conductive deep fluid (4400 μS cm^{-1}) which rises up through microfractures. Thus, the well water is a mixed fluid and its conductivity is determined by the content ratio of the two different mixed components. Under steady state conditions, this ratio is 87 per cent fresh water to 13 per cent deep fluid, resulting in a conductivity of 1350 μS cm^{-1} as measured in the well water flowing out at the surface. The characteristic radius of the mixing area, b, and the effective thickness of the fracture zone, h, are two key parameters governing the duration of conductivity anomalies induced by local head changes, see eq. (20).

There are no constraints on the structure of the fracture zone. For simplicity, we consider an axisymmetric geometry. Under steady state conditions, there is a radial flow through the fracture zone into the borehole. The flow starts at a distant place with a conductivity of $\sigma_f \sim 900\ \mu$ S cm^{-1}. In an area around the borehole, there is a distributed contribution from the rising deep fluid with a conductivity value $\sigma_m \sim 4400\ \mu$ S cm^{-1}. When the groundwater mixture arrives at the borehole, it has a shallow groundwater content $f \sim 0.87$ and a deep fluid content $m = 1 - f \sim 0.13$, so that its conductivity is given by

$$\sigma_o = f\sigma_f + m\sigma_m \sim 1350\,\mu\text{S cm}^{-1}, \tag{1}$$

as observed on average. The validity of the linear mixing law was justified by Woith *et al.* (2003b).

The conductivity drops in general 70 min after an earthquake. Woith *et al.* (2003a) explained this time delay by the flow time of the well water from the fracture depth of 80 m to the sensor at the surface. Additionally the conductivity shows a spoon-like signal form, quite different from the monotonically decaying trend of the discharge. As will be seen, this can be explained by time delays of the flow from a finite mixing area near the borehole.

There are no indications of a strongly inhomogeneous medium beneath the fracture zone. Therefore, we suppose that as we get closer to the borehole, the more deep fluid rises up because each artesian well represents a pore pressure minimum. We define $q_m(r)$ as the injection rate (volume per unit area and per unit time, i.e. the same unit as velocity) of the fluid into the macrofracture, where r is the distance to the borehole axis. Through several forward modellings, we have found that a Gaussian geometry for the injection distribution is a simple and good compromise for fitting the data:

$$q_m(r) = m\frac{Q_o}{\pi b^2}e^{-r^2/b^2}, \tag{2}$$

where b is the characteristic radius of the mixing area, and Q_o is the mean well discharge. The coefficient of the distribution, $m(Q_o/\pi b^2)$, is determined from the conservation condition for the deep fluid,

$$mQ_o = 2\pi\int_0^\infty q_m(r)r\,dr. \tag{3}$$

If we assume that both groundwaters are incompressible and have the same density, then the rate of flow through the fracture, defined by $v(r)$, satisfies the following continuity equation:

$$-\frac{1}{r}\frac{\partial}{\partial r}[r\,v(r)] = \frac{1}{h}q_m(r), \tag{4}$$

where h is the effective thickness of the fracture zone. The solution of eq. (4) is given by

$$v(r) = \frac{Q_o}{2\pi hr}\left(f + me^{-r^2/b^2}\right), \tag{5}$$

where f and m express the contributions of the shallow groundwater and the deep fluid respectively. According to the linear mixture theory, the conductivity parameter can be treated equivalently as the content of any hydrochemical composition. In this case, the conductivity of the flowing groundwater mixture in the fracture zone, $\sigma(r)$, is governed by the equation

$$-\frac{1}{r}\frac{\partial}{\partial r}[r\,v(r)\sigma(r)] = \frac{\sigma_m}{h}q_m(r). \tag{6}$$

Its solution is given by

$$\sigma(r) = \frac{f\sigma_f + m\sigma_m e^{-r^2/b^2}}{f + me^{-r^2/b^2}}, \tag{7}$$

that satisfies the conditions $\sigma(r) \to \sigma_f$ for $r \gg b$ (distant from the well) and $\sigma(r) \to f\sigma_f + m\sigma_m$ for $r \to 0$ (near the well).

3.4 Modelling of a perturbed state

When a head change in the aquifer is induced, all groundwater parameters defined above will be perturbed and become time dependent, $q_m(r) \to q_m(r, t)$, $v(r) \to v(r, t)$, $\sigma(r) \to \sigma(r, t)$, and $Q_o \to Q(t)$. As has been shown by the productivity test and also by the co-seismic discharge response to the Izmit earthquake, the time needed for pressure readjustment in the fracture zone is within a few tens of minutes. If we neglect effects due to this time delay, i.e. if we assume a perfect hydraulic property for the fracture zone, the flow there can be seen as quasi-static, and the conservation condition for the fracture fluid reads

$$-\frac{1}{r}\frac{\partial}{\partial r}[r\,v(r, t)] = \frac{1}{h}q_m(r, t). \tag{8}$$

In contrast, the conductivity of the flowing groundwater mixture does not respond hydraulically, but is governed by the transient transport equation,

$$\frac{\partial}{\partial t}\sigma(r, t) - \frac{1}{r}\frac{\partial}{\partial r}[r\,v(r, t)\sigma(r, t)] = \frac{\sigma_m}{h}q_m(r, t). \tag{9}$$

We are interested in the following perturbations:

$$\delta q_m(r, t) = q_m(r, t) - q_m(r), \tag{10}$$

$$\delta v(r, t) = v(r, t) - v(r), \tag{11}$$

$$\delta\sigma(r, t) = \sigma(r, t) - \sigma(r). \tag{12}$$

Using eqs (4), (6) and (8), and neglecting the second-order terms, we derive from eq. (9) that

$$\begin{aligned}\frac{\partial}{\partial t}\delta\sigma(r, t) - \frac{1}{r}\frac{\partial}{\partial r}[r\,v(r)\delta\sigma(r, t)] &= \frac{\sigma_m - \sigma(r)}{h}\\ &\times\left(\delta q_m(r, t) - \frac{q_m(r)}{v(r)}\delta v(r, t)\right).\end{aligned} \tag{13}$$

In the following, we will consider a situation in which the induced groundwater flow has the same spatial pattern as the steady state, that is

$$\delta q_m(r, t) = \delta m(t)\frac{Q_o}{\pi b^2}e^{-r^2/b^2} \tag{14}$$

and

$$\delta v(r, t) = \frac{Q_o}{2\pi hr}\left(\delta f(t) + \delta m(t)e^{-r^2/b^2}\right), \tag{15}$$

where the functions $\delta f(t)$ and $\delta m(t)$ express the time-dependent contributions from the shallow groundwater and the deep fluid respectively. The induced change in the well discharge is then given by

$$\delta Q(t) = Q_o[\delta f(t) + \delta m(t)]. \tag{16}$$

Note that the three hydraulic variations $\delta f(t)$, $\delta m(t)$ and $\delta Q(t)$ are all induced by the assumed head change. For the highly transmissive fracture zone it is reasonable to suppose that they are correlated with each other and there are no phase shifts between them,

$$\delta m(t) = \alpha\frac{\delta Q(t)}{Q_o}, \quad \delta f(t) = (1-\alpha)\frac{\delta Q(t)}{Q_o}, \tag{17}$$

where α is the correlation parameter to be determined.

Under the above assumptions, the variation in the conductivity is related to the variation in the discharge rate of the well. Without providing the derivation in all its details, we give the solution of eq. (13) for the induced variation in the well-water conductivity by

$$\begin{aligned}\delta\sigma(t) &= \lim_{r\to 0}\delta\sigma(r, t)\\ &= -(m-\alpha)\Delta\sigma\int_0^t\frac{\delta Q(t')}{Q_o}e^{-(t-t')/\tau_o}dt',\end{aligned} \tag{18}$$

where $\Delta\sigma = \sigma_m - \sigma_f = 3500\ \mu$ S cm^{-1}, and

$$\tau_o = \frac{\pi b^2 h}{fQ_o}. \tag{19}$$

Here, $\pi\ b^2\ h$ is the volume of the hydraulically connected pore spaces at the mixing locations, and Q_o is the mean well production. For $f \sim 1$ in the present case, the parameter τ_o expresses the characteristic traveltime of the flow through the mixing area. As will be seen below, it is a key parameter determining the form of the signal of the post-seismic conductivity anomalies.

From eq. (19) we conclude the following necessary site conditions for observing earthquake-induced hydrogeochemical anomalies: (1) an artesian well ($\delta Q, Q_o \neq 0$), (2) a high hydrogeochemical gradient (contrast) in the aquifer ($\Delta\sigma \neq 0$), (3) mixing locations, e.g. macrofractures with a hydraulic connection to the artesian well ($f, m > 0$), and (4) a local head change leading to a change in the mixing ratio ($\alpha \neq m$).

In particular, we think that the earthquake-induced head increases at KAT are localized in the shallow aquifer, probably above the macrofracture zone at 80 m depth. Otherwise we cannot explain why the conductivity, in comparison with the discharge, is less sensitive to earth tides and seasonal head variations. In both latter cases, the pressure changes are believed to be of large spatial scale, that enhance or reduce the discharge of the two different groundwaters more or less symmetrically, so that the mixing ratio is not affected significantly.

3.5 Prediction of the post-seismic conductivity anomalies

As has been stated, the fracture zone is highly transmissive. On a timescale of days to months, the discharge varies linearly with the average head in the aquifer. On the other hand, any head changes will be relaxed by the thereby enhanced or reduced discharge. In this case, the post-seismic relaxation of the discharge can be described by a decaying exponential function,

$$\delta Q(t) = \delta Q_o e^{-t/t_o}, \tag{20}$$

where δQ_o is the co-seismic increase in the discharge rate and t_o is the characteristic relaxation time of the suddenly induced head change.

From eq. (19), the time history of the post-seismic conductivity anomalies is expressed by

$$\delta\sigma(t) = -\delta\sigma_o \frac{e^{-t/t_o} - e^{-t/\tau_o}}{(1 - \tau_o/t_o)\beta(\tau_o, t_o)}, \tag{21}$$

where

$$\delta\sigma_o = (m - \alpha)\Delta\sigma \frac{\delta Q_o}{Q_o}\beta(\tau_o, t_o) \tag{22}$$

is the maximum post-seismic drop of the conductivity, and $\beta(\tau_o, t_o) = (\tau_o/t_o)^{\frac{t_o}{t_o-\tau_o}}$ is the normalization factor of the time function $(e^{-t/t_o} - e^{-t/\tau_o})/(1 - \tau_o/t_o)$, that depends only on the ratio τ_o/t_o.

Given the steady state mixing ratio and the co-seismic rise of the discharge rate, the time history of the conductivity is then determined by three free parameters: (1) t_o for the head relaxation time, (2) τ_o for the traveltime of the flow through the mixing area, and (3) α for the ratio between the induced discharges of the two different groundwaters.

We selected the Izmit event for estimating these three parameters because the data in this case are complete (i.e. both discharge and conductivity were monitored) and for 3 months were unperturbed by other events. The steady state parameters were fixed by $f = 0.87$, $m = 0.13$, $\sigma_o = 1350\ \mu$ S cm^{-1} and $\Delta\sigma = 3500\ \mu$ S cm^{-1}. The co-seismic discharge rise was $\delta Q_o = 25$ per cent of Q_o, corresponding to a head increase of 50 cm (or 5 kPa) in the macrofracture zone. To fit the maximum conductivity drop of ~6 per cent at time $t =$ 21 days and the recovery by ~70 per cent (i.e. from 6 per cent to 1.8 per cent) at $t = 87$ days, we found a good fit to the data for $t_o = 44$ days, $\tau_o = 12$ days and $\alpha = -0.022$. The fitting curve is shown in Fig. 4. The negative α value means that the Izmit earthquake

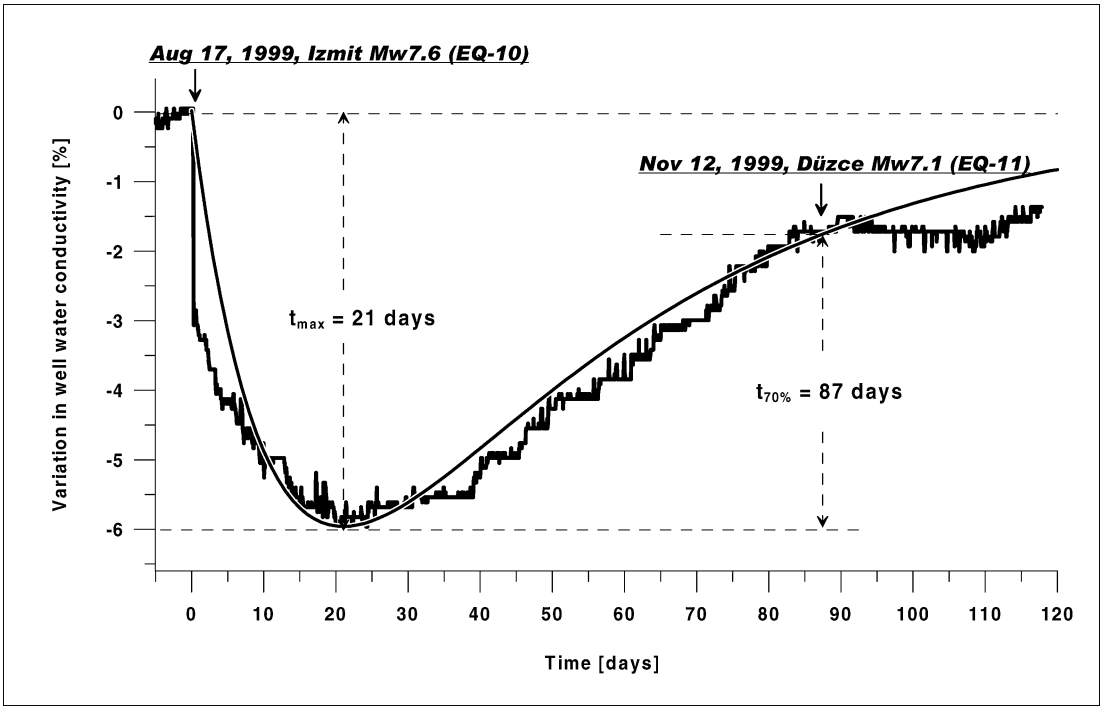

Figure 4. Variation in the specific electrical conductivity of the KAT well water induced by the Izmit earthquake in Turkey on 1999 August 17. The superimposed line represents the predicted response curve according to eq. (22) for $t_o = 44$ days.

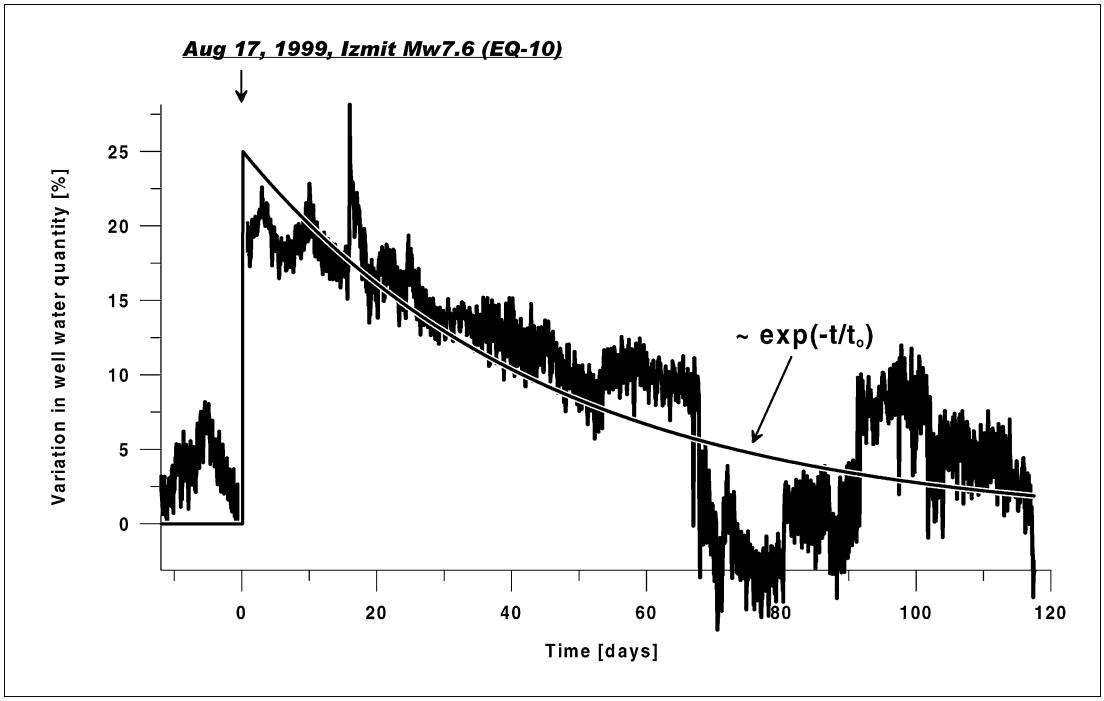

Figure 5. Co-seismic increase and post-seismic relaxation in the KAT well discharge induced by the Izmit earthquake in Turkey on 1999 August 17. The superimposed line represents the predicted relaxation curve according to eq. (21).

increased the discharge of the shallow groundwater but reduced the discharge of the deep fluid. The mixing ratio was shifted from f:m = 87:13 per cent up to

$$\frac{f+(1-\alpha)\delta Q_o/Q_o}{1+\delta Q_o/Q_o} : \frac{m+\alpha\delta Q_o/Q_o}{1+\delta Q_o/Q_o} \sim 90:10 \text{ per cent} \qquad (23)$$

after this event.

Though the head relaxation time $t_o = 44$ days is determined by fitting the conductivity data, it fits the discharge data too (Fig. 5),showing that the different time histories of the two well-water parameters are consistent. In the following, we will simulate the complete time-series of the conductivity shown in Fig. 6(a). Because of the incomplete discharge data, the maximum conductivity drops cannot be calculated by eq. (24) for all 11 earthquakes listed in Table 1. They will be fitted for fixed time constants t_o and τ_o.

At present, $\beta(\tau_o, t_o) \sim 0.61$ and $(1 - \tau_o/t_o)\beta(\tau_o, t_o) \sim 0.45$. The theoretical time-series including all anomalies induced by the 11 earthquakes is then expressed by

$$\delta\sigma(t) = -\sum_{i=1}^{11} \delta\sigma_{o,i} \frac{e^{-(t-t_i)/44} - e^{-(t-t_i)/12}}{0.45} H(t-t_i), \qquad (24)$$

where $\delta\sigma_{o,i}$ is the maximum conductivity drop caused by the ith earthquake, $t - t_i$ is the time in days since this event and $H(t - t_i)$ is the Heaviside unit function. The normalized time function $(e^{-x/44} - e^{-x/12})/0.45$ $(x > 0)$ has its maximum value 1 at $x = 21$.

To fit the observed post-seismic anomalies (Fig. 6a), all maximum conductivity drops $\delta\sigma_{o,i}$ $(i = 1, \ldots, 11)$ were first determined by the least-squares method. Only for a few events (EQ 1, 2, 6) did the fits have to be manually fine-tuned to correct overestimates due to apparently 'non-seismic' anomalies. The final results are given in Table 1. Fig. 6(b) shows the predicted complete time-series, and Fig. 6(c) shows that if the modelled anomalies are removed, the variance of the conductivity data can be reduced by a factor of two to three. The success of the simulation confirms quantitatively the reproducibility of the hydrogeochemical response to the earthquakes.

However, the sharp co-seismic offsets in the conductivity, such as found in the cases of EQ 2, 4, 7 and 10, cannot be accounted for by the present model. This is because the model assumes that the two different groundwaters have mixed before they enter the borehole. The predicted time history is therefore continuous and smooth. Some fracture branches probably exist which are impermeable to the deep fluid. Part of the shallow water may flow from there directly into the borehole. Any co-seismic variation in the contribution from such fractures will cause a correlated change in the conductivity. Thus, the sudden drop in the conductivity accompanying the co-seismic rise in the discharge can be explained. Neglecting such co-seismic effects, the residual conductivity curve for the last 2 yr is nearly a straight line. The cause for the still very large variation in the first 1.5 yr is not known.

3.6 The response to earth tides

In general, different groundwater bodies will show different poroelastic responses to the tidal strain. Consequently, not only the flow rate of the groundwater mixture in the fracture zone but also its hydrogeochemical composition will show tidal fluctuations. If we still assume a linear correlation between the induced discharges of the two different shallow groundwaters (see eqs (17) and (18)), the model described above can also be applied to earth tides in the well-water conductivity.

The Fourier transform of eq. (19) is

$$\delta\tilde{\sigma}(i\omega) = -\frac{(m-\alpha)\Delta\sigma}{i\omega\tau_o + 1} \cdot \frac{\delta\tilde{Q}(i\omega)}{Q_o}, \qquad (25)$$

where $\tilde{\sigma}(i\omega)$ and $\tilde{Q}(i\omega)$ are the Fourier transforms of the conductivity and discharge variations respectively, ω is the angular frequency of earth tides and $i = \sqrt{-1}$. Contrary to the changes in pore pressure induced by shaking, which are believed to be localized in

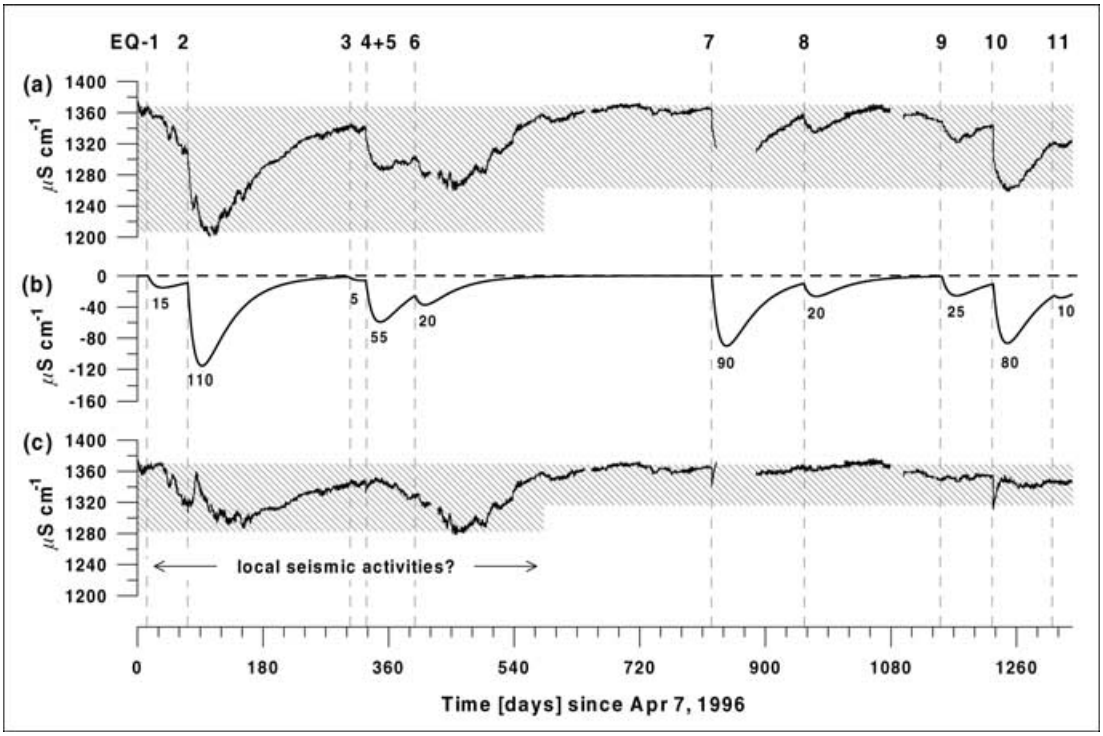

Figure 6. Earthquake-induced anomalies in the specific electrical conductivity of the KAT well water. (a) Observational time-series. (b) Predicted post-seismic anomalies according to eq. (25). (c) Residual time-series.

the shallow aquifer, the tidal changes are due to variations in the confined pressure upon the whole aquifer. In other words, the influence of tidal strain on the two different groundwater bodies is more or less symmetrical. Therefore, the parameter α here may take a different value from the -0.022 estimated from the earthquake-induced anomalies. Note that α:$(1-\alpha)$ is the mixing ratio between the induced discharges of the two groundwaters, in comparison with the steady state mixing ratio m:$(1-m) = m$:f. Obviously, when $\alpha = m$, i.e. when the aquifer responds in such a way to the tidal strain that the mixing ratio remains the same as in the steady state, we could not observe any effects of earth tides on the well-water conductivity. When the contrast between the poroelastic responses of the two groundwater bodies is not extremely large, we may suppose that α takes a value between 0 and 1. This means, other than a seismically induced process, that the tidally induced discharges of the two groundwaters may have different amplitudes but are always of the same sign. Then, the relative amplitude ratio between the conductivity and discharge for the main earth tidal band is estimated by

$$\left|\frac{\delta\tilde{\sigma}(i\omega)/\sigma_o}{\delta\tilde{Q}(i\omega)/Q_o}\right| = \left|\frac{(m-\alpha)}{\sqrt{1+(\omega\tau_o)^2}}\frac{\Delta\sigma}{\sigma_o}\right|. \tag{26}$$

For diurnal tides this has a value of $\leq 3.0 \times 10^{-2}$ and for semi-diurnal tides it is $\leq 1.5 \times 10^{-2}$. The maximum signal ratios are obtained by taking $\alpha = 1$, implying that earth tides only affect the deep aquifer.

If the maximum conductivity amplitudes in 1996 are compared with the maximum discharge amplitudes in 1998 (see Fig. 2), this ratio is about 5.0×10^{-2} for both the main diurnal and semi-diurnal tides, which is of the same order as estimated here. However, when the comparison is made for the monitoring period 1998–1999, for which both discharge and conductivity data are available, the signal ratio decreases down to 0 because the tidal fluctuations in the conductivity nearly disappeared during this time.

In comparison, the Izmit earthquake caused a decrease of 6 per cent in the conductivity and an increase of 25 per cent in the discharge, i.e. a relative signal ratio of 1/4, which is at least one order larger than the signal ratio shown due to earth tides. This is additional evidence for the dynamic mechanism of the earthquake-induced hydrogeological changes at the KAT site.

4 DISCUSSION AND CONCLUSIONS

We have presented a groundwater mixing model that is able to give a complete explanation for the anomalies observed at the KAT artesian well. The repeatedly occurring post-seismic anomalies in the well-water conductivity are due to the special conditions at the observation site: a confined aquifer with a high contrast in the hydrogeochemical composition between two different groundwater bodies and a macrofracture as the mixing zone which is hydraulically connected to the artesian well. When the pressure in the aquifer is perturbed, the mixing ratio of the two different groundwaters will in general be perturbed too. Consequently, not only the discharge of the well but also the composition parameters of the well water, and therefore the electrical conductivity, will show anomalies. In the monitoring period 1996–1999, at least eight post-seismic anomalies related to earthquakes at distances up to 1400 km away were observed at the KAT well. All these anomalies led to significant drops in the conductivity and have a reproducible time characteristic.

This kind of post-seismic groundwater anomaly is believed to be induced by seismic ground shaking rather than static strain, but the physical mechanism involved is not clear yet. There are several indications that the groundwater at the KAT site is partly saturated with CO_2 gas. A gas bubble content of a few per cent can be seen

in the well water flowing out. Therefore, the free gas in the shallow aquifer may play a key role in the present case because mobilization of gas bubbles may induce the head changes in three ways: (1) readjustment of the head gradient due to increased permeability by removing the bubbles from the pore space (Roeloffs 1998), (2) advective overpressure due to rising of the gas bubbles (Steinberg *et al.* 1989; Sahagian & Proussevitch 1992), and (3) triggering of the degassing of local oversaturated fluids. All three processes may happen repeatedly in places where gas-rich fluids are steadily produced, and can explain the reproducible hydrogeological responses to earthquakes. A discrimination between the three mechanisms, however, is not possible from the present observations.

On the other hand, however, it is known that a small free-gas content (for example, a few tenths of a per mille) in the pore space can dramatically reduce the response of the pore pressure to earth tides (Bredehoeft 1967; Hsieh *et al.* 1987; Westerhaus & Zschau 1989; Westerhaus 1996). The question is then how can the KAT well water with a gas content of a few per cent still show strong earth tides? We think that gas bubbles exist only in the shallow region and are probably restricted to some localized places in the macrofracture zone at the 80 m depth where the deep fluid rises up and joins the shallow groundwater flow. In the deeper region the gas should be dissolved because of the high ambient pressure there. If the whole aquifer volume is considered, the average free-gas content is still very low.

The model presented in this paper pre-supposes that the coseismic head increases independently of the physical cause. The spoon-like post-seismic trends of the conductivity can be predicted by assuming a Gaussian distribution for the mixing locations around the borehole. In this case, the time histories are described by the difference of two decaying exponential functions whose time constants are the head relaxation time t_o and the traveltime τ_o for the groundwater flow through the mixing area respectively. All significant responses to eight of the 11 local and distant large earthquakes, namely EQ 2, 4, 6, 7, 8, 9, 10 and 11, could be well fitted using the uniform time constants $t_o = 44$ days and $\tau_o = 12$ days. On average, these earthquake-induced anomalies explain 50–70 per cent of the conductivity variations observed at this artesian well.

There are several reasons why the conductivity of the KAT well water was very sensitive to distant large earthquakes. First, the coseismic head changes are persistent for weeks to months and can have a magnitude several times larger than the amplitude of tidal fluctuations. Additionally, if such head changes are due to mobilization of gas bubbles, they should be localized in the shallow aquifer above the depth where the partial pressure of the gas is higher than the surrounding pore pressure. All these promote shifting of the mixing ratio in favour of the fresh groundwater and result in drops in the well-water conductivity.

It is noticeable that different groundwater parameters at the same well may show different response characteristics to local changes in the pore pressure. For the water level in a non-artesian well or the discharge of an artesian well, the response time histories are controlled by diffusion of the changes in pore pressure and therefore depend on the hydraulic properties of the aquifer. For the chemical parameters as well as the temperature of the groundwater flowing out from an artesian well, however, the response time histories may additionally be modified by the discharge rate of the well. In general, a low discharge rate causes a long rise time of the anomalies induced in such parameters. The signal-to-noise ratio may thereby be reduced and the signals of sequential events can easily overlap with each other. On the other hand, a high discharge rate may affect the confinement of the aquifer and reduce the response sensitivity of these parameters, too. Therefore, an optimal discharge rate should be tested with respect to multiparameter monitoring.

ACKNOWLEDGMENTS

The monitoring data were obtained in the frame of the READINESS project in cooperation between the National Survey for Seismic Protection, Yerevan, and the GeoForschungsZentrum Potsdam. Many thanks are due to the technical staff of both institutions. We are grateful to H.-J. Kümpel, M. Westerhaus, F. Roth and B. Lühr for suggestions and discussions. We thank two refrees, Y. Chen and E. E. Brodsky, for valuable comments and improvements.

REFERENCES

Bredehoeft, J.D., 1967. Response of well-aquifer systems to Earth tides, *J. geophys. Res.,* **72**, 3075–3087.

Brodsky, E.E., Roeloffs, E., Woodcock, D., Gall, I. & Manga, M., 2003. A mechanism for sustained groundwater pressure changes induced by distant earthquakes, *J. geophys. Res.,* **108**(B8), 2390, doi:10.1029/2002JB002321.

Grecksch, G., Roth, F. & Kümpel, H.-J., 1999. Coseismic well-level changes due to the 1992 Roermond earthquake compared to static deformation of half-space solutions, *Geophys. J. Int.,* **138**, 470–478.

Hsieh, P.A., Bredehoeft, J.D. & Farr, J.M., 1987. Determination of aquifer transmissivity from Earth tide analysis, *Water Resource Res.,* **23**, 1824–1832.

Igarashi, G. & Wakita, H., 1991. Tidal responses and earthquake-related changes in the water level of deep wells, *J. geophys. Res.,* **96**, 4269–4278.

Kitagawa, Y. & Koizumi, N., 1996. Comparison of post-seismic groundwater temperature changes with earthquake-induced volumetric strain release: Yudani hot spring, Japan, *Geophys. Res. Lett.,* **23**, 3147–3150.

Kitagawa, Y. & Matsumoto, N., 1996. Detection of coseismic changes of underground water level, *J. Am. Statist. Assoc.,* **91**, 521–528.

Mogi, K., Mochizuki, H. & Kurokawa, Y., 1989. Temperature changes in an artesian spring at Usami in the Izu Peninsula (Japan) and their relation to earthquakes, *Tectonophysics,* **159**, 95–108.

Muir-Wood, R. & King, G.C.P., 1993. Hydrological signatures of earthquake strain, *J. geophys. Res.,* **98**, 22 035–22 068.

Ohno, M., Wakita, H. & Kanjo, K., 1997. A water well sensitive to seismic waves, *Geophys. Res. Lett.,* **24**(6), 691–694.

Quilty, E. & Roeloffs, E., 1997. Water level changes in response to the December 20, 1994 M4.7 earthquake near Parkfield, California, *Bull. seism. Soc. Am.,* **87**, 310–317.

Roeloffs, E., 1998. Persistent water level changes in a well near Parkfield, California, due to local and distant earthquakes, *J. geophys. Res.,* **103**, 869–889.

Rojstaczer, S. & Wolf, S., 1992. Permeability changes associated with large earthquakes: an example from Loma Prieta, California, *Geology,* **20**, 211–214.

Rojstaczer, S., Wolf, S. & Michel, R., 1995. Permeability enhancement in the shallow crust as a cause of earthquake-induced hydrological changes, *Nature,* **373**, 237–239.

Sahagian, D. & Proussevitch, A., 1992. Bubbles in volcanic systems, *Nature,* **359**, 485.

Steinberg, G.S., Steinberg, A.S. & Merzhanov, A.G., 1989. Fluid mechanism of pressure rise in volcanic (magmatic) systems with mass exchange, *Mod. Geol.,* **13**, 275–281.

Sterling, A. & Smets, E., 1971. Study of earth tides, earthquakes and terrestrial spectroscopy by analysis of the level fluctuations in a borehole at Heibaart (Belgium), *Geophys. J. R. astr. Soc.,* **23**, 225–242.

Wakita, H., 1975. Water wells as possible indicators of tectonic strain, *Science,* **189**, 553–555.

Westerhaus, M., 1996. Tilt and well level tides along an active fault—a contribution to the Turkish-German Joint Project on Earthquake Research, PhD thesis, University of Kiel.

Westerhaus, M. & Zschau, J., 1989. Tidal tilt modification at the western end of the North-Anatolian Fault Zone: an indication for slow changes of crustal properties, in, *Turkish-German Earthquake Research Project*, pp. 82–108, eds Zschau, J. & Ergunay, O., Kiel University, Kiel.

Woith, H., Milkereit, C., Zschau, J., Maiwald, U. & Pekdeger, A., 1998. Monitoring of thermal and mineral waters in the frame of READINESS, in, *Water Rock Interaction*, Vol. WRI-9, pp. 809–812, eds Arehard, G.B. & Hulston, J.R., Balkema, Rotterdam.

Woith, H., Wang, R., Milkereit, C., Zschau, J., Maiwald, U. & Pekdeger, A., 2001. Response of an artesian well in southern Armenia to the 1400 km distant Izmit earthquake of August 17, 1999, in, *Water Rock Interaction*, Vol. WRI-10, pp. 115–118, ed. Cidu, R., Swets & Zeitlinger, Lisse.

Woith, H., Wang, R., Milkereit, C., Zschau, J., Maiwald, U. & Pekdeger, A., 2003a. Heterogeneous response of hydrogeological systems to the Izmit and Düzce (Turkey) earthquakes of 1999, *Hydrogeol. J.* **11** (1),113–121.

Woith, H., Wang, R., Milkereit, C., Igumnov, V.A., Maiwald, U., Pekdeger, A. & Zschau, J., 2003b. A hydrogeochemical mixing model for compositional groundwater anomalies induced by distant earthquakes, *J. geophys. Res.,* submitted.